$$\varphi_1(t) = \exp[(P_A/2P_x)(1 - e^{-P_x t})],$$

$$\varphi_0(t) = \exp[(3P_A/2P_x)(1 - e^{-P_x t})] \times \exp[(P_A/4P_x)(1 - e^{-2P_x t})].$$

Then

$$\chi_0(t) = [a_{i2} + a_{i1}\varphi_1(t) + a_{i0}\varphi_0(t)]e^{-(P_A+P_R)t}. \qquad (A4)$$

The total Auger transition rate P_A^1 (corrected for partial population of the 1*s* state) can be determined from the equation

$$\chi_R(\infty) \equiv \frac{P_R}{(P_A^1 + P_R)} = P_R \int_0^\infty \chi_0(t)\, dt\ . \qquad (A5)$$

The population of the electron 1*s* state when the muon reaches the state *f* is given by

$$a_{f2} = P_R \int_0^\infty [a_{i2} + a_{i1}(1 - e^{-P_x t})\varphi_1(t) + a_{i0}(1 - e^{-P_x t})^2 \varphi_0(t)]e^{-(P_A+P_R)t}\, dt\ , \qquad (A6)$$

$$a_{f1} = \int_0^\infty \{P_A a_{i2} + a_{i1}\varphi_1(t)[(P_R - P_A)e^{-P_x t} + P_A] + a_{i0}\varphi_0(t) \times [P_R(1 - e^{-P_x t})e^{-P_x t} + P_A(1 - e^{-P_x t})^2\}e^{-(P_A+P_R)t}\, dt, \qquad (A7)$$

$$a_{f0} = \int_0^\infty \{a_{i1}\varphi_1(t)\tfrac{1}{2}P_A e^{-P_x t} + a_{i0}\varphi_0(t)e^{-P_x t} \times [P_R + \tfrac{1}{2}P_A(1 - e^{-P_x t})]\}e^{-(P_A+P_R)t}\, dt\ . \qquad (A8)$$

The average number of 1*s* electrons actually present during the muonic radiative $i \to f$ transition is

$$\bar{n}_{i\to f} = 2a_{f2} + a_{f1} + [P_A^1/(P_A^1 + P_R)]\ . \qquad (A9)$$

---

*Work performed under the auspices of the U. S. Atomic Energy Commission under Contract No. AT (04-3)-63.

[1] G. Backenstoss *et al.*, Phys. Letters 31B, 233 (1970).

[2] M. S. Dixit *et al.*, Phys. Rev. Letters 27, 878 (1971).

[3] I. Blomquist (unpublished).

[4] G. A. Rinker and M. Rich, Phys. Rev. Letters 28, 640 (1972).

[5] H. Backe *et al.*, Nucl. Phys. A189, 472 (1972).

[6] H. L. Anderson, in *Proceedings of the Third International Conference on High-Energy Physics and Nuclear Structure* (Plenum Press, New York, 1970).

[7] B. Fricke, Nuovo Cimento Letters 2, 859 (1969).

[8] E. C. Seltzer, Phys. Rev. 188, 1916 (1969).

[9] A. M. Desiderio and W. R. Johnson, Phys. Rev. A 3, 1267 (1971).

[10] Y. Eisenberg and D. Kessler, Nuovo Cimento 19, 1195 (1961).

[11] A. H. de Borde, Proc. Phys. Soc. (London) A67, 57 (1954).

[12] J. H. Scofield, Phys. Rev. 179, 9 (1969).

PHYSICAL REVIEW A VOLUME 7, NUMBER 1 JANUARY 1973

Excited Electronic States of O_2^-

M. Krauss* and D. Neumann
National Bureau of Standards, Washington, D. C. 20234

and

A. C. Wahl,† G. Das, and W. Zemke
Argonne National Laboratory, Argonne, Illinois 60439

(Received 8 September 1972)

Excited electronic states of the O_2^- molecule have been calculated with configuration-interaction (CI) variational trial functions that assure formally correct asymptotic behavior as well as the single-configuration self-consistent-field (SCF) approximation. CI results were obtained by both multiconfiguration self-consistent-field (MC-SCF) and pseudonatural orbital (PNO) techniques. The MC-SCF results are most accurate and are used to analyze the energy curves and wave functions of these states for internuclear separations larger than 3 a.u. All the excited states are found to have equilibrium-internuclear separations at least 1 a.u. larger than the ground state. The two lowest energy states, the $^4\Sigma_u^-$ and $^2\Pi_u$, are characterized, respectively, as shape and valence Feshbach resonances. They are sufficiently bound to make it likely they play a role in low-energy-electron scattering by oxygen.

I. INTRODUCTION

The experimental and theoretical understanding of the excited states of O_2^- is very limited. Simple adiabatic correlation rules determine that 24 energy curves arise from the interaction of ground state $O(^3P)$ and $O^-(^2P)$. Of all these energy curves only the ground state $X^2\Pi_g$ of the ion has been studied extensively. In particular, there has been a considerable experimental effort toward the determination of the electron affinity of O_2.[1] A recent calculation has also shown that an accurate electron affinity can also be obtained theoretically.[2] Direct evidence of the excited states of O_2^- is obtained from the fluorescence spectra of O_2^- in alkali halide crystals,[3] and from the dissociative attachment of electrons to O_2.[4] In both cases the upper state has been discussed in terms of an excited $^2\Pi_u$ state but there is a supporting theoretical analysis only in the case of dissociative attachment.[5] There have also been molecular-orbital speculations[6] which emphasize a possible $^4\Sigma_u^-$ metastable state and, in addition, considers $^2\Delta_u$, $^2\Pi_u$, and $^4\Sigma_g^-$ states. Only recently have actual calculations been reported for the excited states.[7]

Although it is quite difficult to obtain detailed experimental information for the excited states of a negative ion, the ability to calculate such states has improved considerably in recent years. The analysis of the ground-state energy[2] $^2\Pi_g$ was based upon a superposition of configurations trial function. Such configuration interaction (CI) can be implemented in a number of ways, and in this present study, two techniques will be used which have been designated optimized valence configuration (OVC)[8] and pseudonatural orbital (PNO) configuration interaction.[9] The multiconfiguration (MC)-self-consistent-field (SCF) technique is used in the OVC studies to determine only the correlation energy in the valence shell which *varies strongly* as the atoms combine from infinite separation. The main purpose of this study was to extend these techniques in a prelimary analysis of all the energy curves of O_2^-.

The first step consisted of calculating an energy curve for a dominant single configuration (SC) by a self-consistent-field calculation, namely, a restricted Hartree–Fock (HF) calculation.[10] Although such SC-SCF energy curves can have severe asymptotic difficulties, the equilibrium internuclear separations are usually correctly predicted, and the excited O_2^- states are found to have equilibrium distances much larger than that for the $X\,^2\Pi_g$ state. This is physically reasonable and suggests an economical approach for the calculation of all the O_2^- states via the OVC philosophy in which a base function is defined as the *minimum* number of configurations required to yield formally correct dissociation into HF atoms.[8] Such a base function includes the electrostatic and ion-induced interactions. At the larger internuclear distances, which are those important for the O_2^- excited states, other correlation-energy changes accompanying bond formation are relatively unimportant except for exchange coupling that mixes configurations arising from the $O^- + O(^1D)$ interaction with the $O^- + O(^3P)$ base functions. The easiest way to include such an interaction is to mix the valence-type configurations obtained from all combinations of $3\sigma_g$, $3\sigma_u$, $^1\Pi_u$, and $^1\Pi_g$ molecular orbitals. The correlation behavior at shorter distances can be examined along the lines developed[2] for the $X\,^2\Pi_g$ state within an OVC scheme as interest in this region develops from experimental sources.

Section II of this paper discussed the three methods used in this study, namely, the SCF, the PNO-CI, and the MC-SCF-OVC scheme. In Sec. III the results for each state studied are presented and analyzed, and Sec. IV summarizes the major conclusions of this work.

II. METHODS

A. Single-Configuration Self-Consistent-Field Method

In this model, the variational calculation for the negative ion is performed on a configuration constructed by adding an electron to a target configuration and recoupling to a symmetry-adapted negative-ion state. When the negative-ion state is not bound in a given range of internuclear distances then the variation can yield the target state and a constant or zero-energy continuum orbital.[11] However, if the attached electron is placed into a multiply occupied degenerate orbital, then the reference target state is one for which the orbital has zero occupancy. The resulting negative-ion SC-SCF states are then well defined relative to the neutral target states, since such ionized states usually have high energies. These states will support shape resonances[12] with narrow widths. In this study, attachment of a single electron will be considered in the SC-SCF model only at distances sufficiently large, so that the ion energies are lower than the neutral ones. Therefore, SCF calculations were completed for the following single configurations which all have a common core, $1\sigma_g^2 1\sigma_u^2 2\sigma_g^2 2\sigma_u^2$:

$$1\pi_u^4 3\sigma_g^2 1\pi_g^3\,, \qquad X\,^2\Pi_g\,;$$

$$1\pi_u^4 3\sigma_g 1\pi_g^3 3\sigma_u\,, \quad ^4\Pi_u\,, \quad ^2\Pi_u\,;$$

$$1\pi_u^3 3\sigma_g^2 1\pi_g^4\,, \qquad ^2\Pi_u\,;$$

$$1\pi_u^4 3\sigma_g 1\pi_g^4\,, \qquad ^2\Sigma_g^+\,;$$

$$1\pi_u^4 3\sigma_g^2 1\pi_g^2 3\sigma_u\,, \quad ^4\Sigma_u^-\,, \quad ^2\Delta_u\,, \quad ^2\Sigma_u^-\,, \quad ^2\Sigma_u^+\,.$$

Both Slater-type functions (STF)[13] and Gaussian-type functions (GTF)[14] were used. The STF basis uses an atom basis at the O atom HF level[15] augmented by two *d* functions on each atom. The GTF basis used the 9*s*, 5*p* atom basis of Huzinaga.[16] The energy results are given in Tables I and II. For comparison sake selected neutral O_2 energies for the $\pi_g^2(X\,^3\Sigma_g^-, {}^1\Delta_g, {}^1\Sigma_g^+)$ states are also tabulated.

As is now well known, the SCF approximation suffers from a major difficulty; with very few exceptions energy curves calculated in this approximation behave incorrectly asymptotically. Only the $^4\Delta$ states behave formally correct asymptotically; at large distances the SCF energies are very deceptive in determining which adiabatic curves

TABLE I. SCF energy curves: STF O_2 and O_2^-.

State[a]		$-E(R) = 148 + $ (a.u.)					
	R 2.0	2.282	3.0	4.0	5.0	6.0	8.0
O_2 $^3\Sigma_g^-$	1.626 40	1.647 55	1.487 44	1.261 77	1.126 17	1.050 38	0.980 35
$^1\Delta_g$	1.579 10	1.600 35	1.442 14	1.218 71	1.084 34	1.009 17	0.939 59
$^1\Sigma_g^+$	1.53270	1.553 89	1.397 38	1.176 12	1.042 95	0.968 39	0.899 24
O_2^- $^2\Pi_g$	1.520 81	1.609 96	1.563 98	1.414 21	1.311 91	1.252 19	1.179 74
$^2\Sigma_g^+$	1.159 31	1.351 84	1.494 30	1.485 76	1.453 77	1.432 15	1.414 10
$^4\Pi_u$	0.709 55	1.048 27	1.441 31	1.531 62	1.532 02	1.526 64	1.522 13
$^2\Pi_u$		0.937 13	1.351 86	1.451 82	1.454 39	1.449 53	1.445 21
$^4\Sigma_u^-$	1.055 54	1.283 14	1.476 21	1.421 09	1.349 75	1.305 53	1.264 90
$^2\Sigma_u^-$	0.981 92	1.185 88	1.395 84	1.354 09	1.287 75	1.245 78	1.206 74
$^2\Delta_u$	0.981 77	1.205 50	1.406 69	1.358 24	1.289 66	1.246 71	1.206 96
$^2\Sigma_u^+$		1.164 11	1.365 91	1.318 60	1.250 80	1.208 28	1.168 84

[a] The configurations describing the SCF states are (the $1\sigma_g^2 1\sigma_u^2 2\sigma_g^2 2\sigma_u^2$ core is always understood) O_2: $^3\Sigma_g^-$, $^1\Delta_g$ and $^1\Sigma_g^+$, $3\sigma_g^2 1\pi_u^4 1\pi_g^2$; O_2^-: $^2\Pi_g$, $3\sigma_g^2 1\pi_u^4 1\pi_g^3$; $^2\Sigma_g^+$, $3\sigma_g 1\pi_u^4 1\pi_g^4$; $^4\Pi_u$ and $^2\Pi_u$, $3\sigma_g 1\pi_u{}^4 1\pi_g^3 3\sigma_u$; $^4\Sigma_u^-$, $^2\Sigma_u^-$, $^2\Delta_u$ and $^2\Sigma_u^+$, $3\sigma_g^2 1\pi_u^4 1\pi_g^2 3\sigma_u$.

are bound relative to $O + O^-$. Adiabatically, all but one of the relevant O_2^- states should go to ground state $O(^3P) + O^-(^2P)$. The molecular states arising from this atom pair are $^{2,4}\Sigma_g^+$, $^{2,4}\Sigma_u^+$, $(2)^{2,4}\Sigma_g^-$, $(2)^{2,4}\Pi_g$, $(2)^{2,4}\Pi_u$, $^{2,4}\Delta_u$, and $^{2,4}\Delta_g$.

Despite these difficulties SCF curves are still very useful for estimating the equilibrium internuclear distance r_e and the spectroscopic constants of $O_2^-(X\,^2\Pi_g)$. Accordingly, such SCF calculations were performed and the STF-SCF spectroscopic constants are summarized in Table III. The spectroscopic constants were obtained via a Dunham analysis. As is common with SCF calculations the calculated r_e yields somewhat smaller values than the experimental ones, while the calculated ω_e is larger than experimental. Except for the r_e value the spectroscopic constants for the O_2 and O_2^- states are not expected to be correct since the curves do not behave correctly asymptotically as seen in Fig. 1. The $O_2(^3\Sigma_g^-)$ SCF curve goes to an asymptote over 10 eV above the SCF energy of two oxygen atoms while the $O_2^-(^2\Pi_g)$ SCF curve is almost as badly in error.

TABLE II. SCF energy curves: GTF O_2 and O_2^-.

State[a]		$-E(R) = 148 + $ (a.u.)			
	R 2.0	2.4	3.0	3.5	4.0
O_2 $^3\Sigma_g^-$		1.566 62			
$^1\Delta_g$		1.519 35			
$^1\Sigma_g^+$		1.472 91			
O_2^- $^2\Pi_g$	1.424 41	1.561 21	1.530 26	1.460 46	1.394 14
$^2\Sigma_g^+$		1.350 24	1.462 90	1.473 13	1.463 29
$^4\Sigma_u^-$		1.314 17	1.452 44	1.441 46	1.403 88
$^2\Pi_u$	1.008 56	1.297 92	1.394 45	1.381 06	1.347 17

[a] All configurations for the GTF calculations are identical to those given for SCF except for O_2^-: $^2\Pi_u$, $3\sigma_g^2 1\pi_u^3 1\pi_g^4$.

The excited states have an r_e uniformly in the neighborhood of 3.25 a.u. Thus, these preliminary SCF calculations indicated that an analysis of the excited states should emphasize the longer-range region. This occurs because the open-shell configurations have occupied the antibonding $1\pi_g$ and $3\sigma_u$ orbitals. As long as the asymptotic behavior is handled correctly, other correlation effects at these large distances should be relatively unimportant.

The apparent correlation error due to the asymptotic difficulty, however, is considerably different for the neutral and ionic states and among the ionic states. The lowest doublet excited state is the $^2\Sigma_g^+$ state which dissociates formally to a linear combination of neutral singlet states, $\frac{1}{\sqrt{3}}[\sqrt{2}O(^1D) - O(^1S)]$ and the $O^-(^2P)$ state. This indicates the erroneous ordering produced by HF calculations since this state *must* lie above the many states that correlate to the $O(^3P)$ and $O^-(^2P)$ asymptote.

TABLE III. SCF and experimental spectroscopic constants.

State	r_e (a.u.) Calc.	r_e (a.u.) Expt.	ω_e (cm^{-1}) Calc.	ω_e (cm^{-1}) Expt.
$^3\Sigma_g^-$	2.22	2.282	1667	1580
$^2\Pi_g$	2.50	2.534[a]	1499	1089[a]

[a] See Ref. 1.

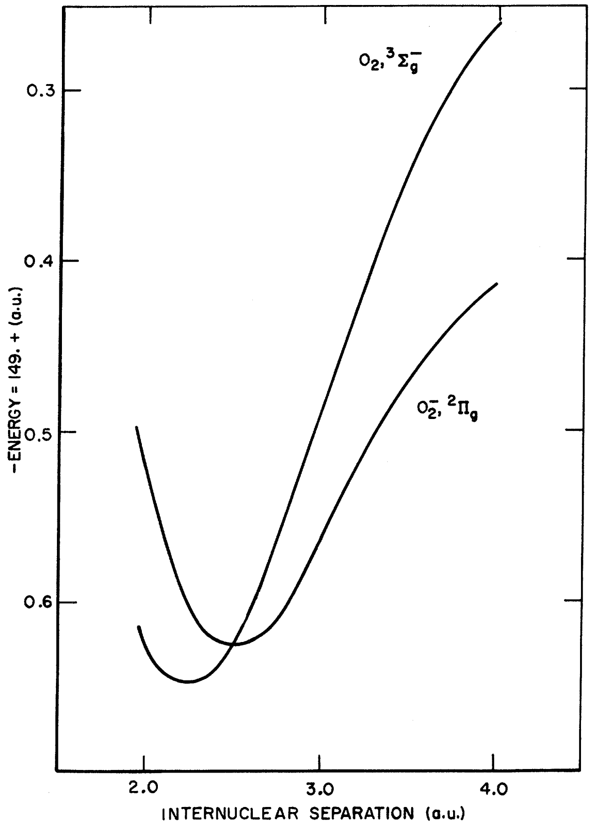

FIG. 1. Hartree–Fock energy curves of the ${}^3\Sigma_g^-$, O_2 and ${}^2\Pi_g$, O_2^- ground states. Both curves exhibit the formally incorrect asymptotic behavior of the HF approximation.

Asymptotically correct dissociation is a *sine qua non* for an analysis of a family of energy curves.

B. Configuration-Interaction Methods

The asymptotic difficulties at the HF level discussed in Sec. II A can be removed by adding a sufficient number of configurations to assure formally correct dissociation into HF atom fragments. In this study the asymptote is determined to be formally $O(^3P) + O^-(^2P)$ with the restriction that the atomic radial functions are identical in both atoms. This level of correlation is achieved by mixing valence functions constructed only out of excitations within the $3\sigma_g$, $3\sigma_u$, $1\pi_u$, and $1\pi_g$ molecular orbitals. Including such configurations can take account of the long-range electrostatic multipole-multipole interaction when the molecular orbitals are constructed with flexible polarization functions. Important correlation effects arising from excitations *out* of the valence shell are not considered here since they are expected to be most important at smaller internuclear separation. This asymptotically correct model should permit a semiquantitative determination of the relative positions of all curves arising from the same asymptote. An examination of these curves then permits a decision about subsequent effort on correlating the states of particular interest.

The present results were obtained by two approximations. The most accurate is to solve the MC-SCF equations.[8] Initial orbital guesses for the calculation of all states was obtained by solving for the HF molecular orbitals for the ${}^4\Delta_g$ state. This HF configuration is formally correct asymptotically since it represents the maximum spin and angular momentum possible from this asymptote. Only three grand iterations were then necessary to converge for all states to internuclear distances as short as 3.0 a.u. This technique permits a relatively quick investigation of a large number of states at moderately large internuclear distances.

Table IV lists all the configurations mixed in both the OVC and PNO-CI calculation. The linear combination of configurations that yield formally correct asymptotic behavior to $O^-(^2P) + O(^3P)$ are given in Table V.

For a number of states there are additional valence-shell configurations arising from $O(^1D)$, for example, which can mix at shorter distances. These configurations can be considered to fall into two categories: The first include those which have the same orbital occupancy as a configuration required asymptotically. Such configurations can be important at shorter distances which implies a substantial recoupling of the angular momentum of the combining atoms. The second type of configuration involves double electron excitations from the dominant asymptotic configurations and can be considered to effect a minor charge redistribution within the valence shell. The energy lowering due to the latter configurations is minor.

The additional correlation configurations become increasingly important as the equilibrium internuclear distance of the ground state is approached. As individual states are discussed the effects of autodetachment will be noted briefly. For the relative behavior of the excited ions at distances greater than 3.0 a.u., only the valence-shell configuration mixing will be reported in this study. Consideration of correlation effects for the ${}^4\Sigma_u^-$ and the ${}^2\Pi_u$ excited states will be considered later.

The energies are given in Tables VI and VII as a function of the internuclear distance. Excited-state energies are given where more than one state of a given symmetry goes asymptotically to the same atoms. These energies are merely the second root of the final secular equation; the molecular orbitals and mixing coefficients were not optimized for the excited state. However, in the case of the excited ${}^2\Sigma_g^+$, the excited state was optimized since this state goes to $O(^1D) + O^-(^2P)$. The accurate MC-SCF en-

TABLE IV. Configurations of valence states. In this Table σ and σ' can represent both the $3\sigma_g$ and $3\sigma_u$ molecule orbitals. Similarly, π and π' can represent both the $1\pi_u$ and $1\pi_g$ molecular orbitals. The configuration descriptions are then representative of both the gerade and ungerade states for a given S, Λ, and Kronig symmetry. The core $1\sigma_g^2 1\sigma_u^2 2\sigma_g^2 2\sigma_u^2$ is understood for all configurations. Symmetry designations in square brackets [ ] refer to the coupling of the partially occupied orbital to its left and the designations in parentheses ( ) refer to the coupling of the two open-shell orbitals to its immediate left. Overall coupling is given in the column designated "state".

State	Configuration no.	Occupancy molecular orbitals σ	σ'	π	π'
$^4\Delta$	1	2	1	3	3
$^4\Pi$	1	1	1	4	3
	2	2	2	3	2
$^4\Sigma^+$	1	2	1	3	3
$^4\Sigma^-$	1	2	1	4	2
	2	1	2	3	3
	3	2	1	2	4
$^2\Delta$	1	2	1	4	$2[^3\Sigma^-]$
	2	2	1	$2[^3\Sigma^-]$	4
	3	1	2	$3(^3\pi)$	3
	4	1	2	$3(^1\pi)$	3
$^2\Pi$	1	2	0	4	3
	2	0	2	4	3
	3	1	$1(^3\Sigma^+)$	3	4
	4	1	$1(^1\Sigma^+)$	3	4
	5	2	2	4	1
	6	2	2	$2[^1\Sigma^+]$	3
	7	2	2	$2[^3\Sigma^-]$	3
	8	2	2	$2[^1\Delta]$	3
$^2\Sigma^+$	1	2	1	4	$2[^1\Sigma^+]$
	2	2	1	$2[^1\Sigma^+]$	4
	3	0	1	4	4
	4	1	2	$3(^3\pi)$	3
	5	1	2	$3(^1\pi)$	3
$^2\Sigma^-$	1	2	1	$3(^3\pi)$	3
	2	2	1	$3(^1\pi)$	3
	3	1	2	4	$2[^3\Sigma^-]$
	4	1	2	$2[^3\Sigma^-]$	4

ergy curves are given in Fig. 2 relative to an asymptote of − 149.521 a.u. which is within ± 0.0015 a.u. of the calculated asymptote for the different states. At least ten of the negative-ion states are bound. The list includes $^4\Delta_g$, $^4\Pi_u$, $^4\Sigma_g^+$, $^4\Sigma_u^-$, $^2\Delta_u$, $^2\Pi_g$, $^2\Pi_u$, $^2\Sigma_u^-$, and $^2\Sigma_u^-$. In addition, the $^4\Sigma_g^-$ and $^4\Pi_g$ states may be slightly bound at very large distances while the $^2\Sigma_g^+$ and $^2\Delta_g$ states are metastable with appreciable barriers at large distances. The minima occur in regions well away from the neutral ground states and such states are not complicated by the possibility of autodetachment in the neighborhood of the equilibrium internuclear separation. At shorter distances the left-hand portion of the energy curves are rapidly rising for all states but the $X^2\Pi_g$, of course, and the $^4\Sigma_u^-$, $^2\Sigma_g^+$, and $^2\Pi_u$ states. It would seem that only these four states can play a role at distances shorter than 3.0 a.u.

TABLE V. Asymptotic configuration description of $O^-(^2P) + O(^3P)$.

State	Configuration coefficient 1	2	3	4	5	6	7	8
$^4\Delta$	1.0							
$^4\Pi(1)$	1.0							
$^4\Pi(2)$		1.0						
$^4\Sigma^+$	1.0							
$^4\Sigma^-(1)$	$1/\sqrt{2}$		$-1/\sqrt{2}$					
$^4\Sigma^-(2)$	$1/2$	$1/\sqrt{2}$	$1/2$					
$^2\Delta$	$\sqrt{3/8}$	$-\sqrt{3/8}$	$-1/4$	$-\sqrt{3/4}$				
$^2\Pi(1)$	$\sqrt{3/8}$	$-\sqrt{3/8}$	$1/2$					
$^2\Pi(2)$					$-\sqrt{3/8}$	$\sqrt{3/4}$	$-1/4$	$\sqrt{3/8}$
$^2\Sigma^+$		$-1/4$	$-\sqrt{3/4}$	$-\sqrt{3/8}$	$\sqrt{3/8}$			
$^2\Sigma^-(1)$	$3/4$	$\sqrt{3/4}$	$-1/2\sqrt{2}$	$1/2\sqrt{2}$				
$^2\Sigma^-(2)$	$1/2\sqrt{2}$	$\sqrt{3/8}$	$1/2$	$1/2$				

III. DISCUSSION OF RESULTS

In the region of 3.0–6.0 a.u. the long-range quadrupole and quadrupole-quadrupole interactions

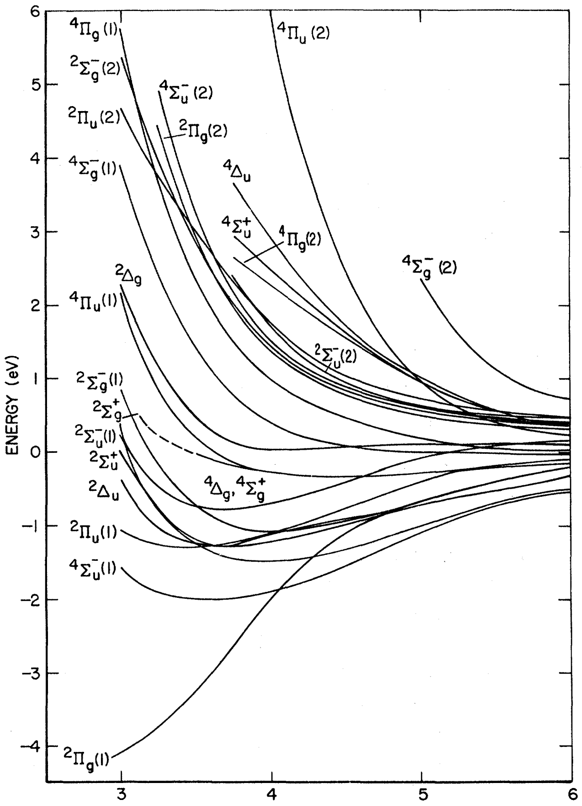

FIG. 2. MC-SCF energy curves for all states of O_2^- that correlate with the $O^-(^2P)$ and $O(^3P)$ asymptote. All curves were drawn relative to a common asymptotic energy of −149.521 a.u. Note that the $^2\Sigma_g^+$ curve exhibits a curve crossing near 3 a.u. due to an energy curve attractive relative to the $O^-(^2P)$ and $O(^1D)$ asymptote.

are already overwhelmed by the exchange coupling and the overlapping of the atoms. This is best seen by noting the predictions of the long-range ion-quadrupole plus ion-induced dipole potential. The interaction energy is given by

$$\Delta E = -Q/2R^3 - \alpha/2R^4 .$$

Limiting values of α and Q for the $^3\Pi$ and $^3\Sigma^-$ components of the O(^3P) state have been obtained recently.[17] α and Q are 4.50 and −0.90 a.u. for $^3\Pi$ and 5.05 and 1.83 a.u. for $^3\Sigma^-$. This results in the following predictions for O$^-$(^2P) interacting with O(^3P):

$^2\Pi \otimes {}^3\Pi \Rightarrow {}^{2,4}\Sigma^+, \Sigma^-, \Delta_{g,u}$ (repulsive),
$^2\Sigma^+ \otimes {}^3\Pi \Rightarrow {}^{2,4}\Pi_{g,u}$ (repulsive),
$^2\Pi \otimes {}^3\Sigma^- \Rightarrow {}^{2,4}\Pi_{g,u}$ (attractive),
$^2\Sigma^+ \otimes {}^3\Sigma^- \Rightarrow {}^{2,4}\Sigma^-_{g,u}$ (attractive).

TABLE VI. MC-SCF energy curves: STF O$_2^-$.

	$-E = 149 +$ a.u.				
State	R 3.0	4.0	5.0	6.0	
$^4\Delta_g$	0.5075	0.5752	0.5577	0.5403	B
$^4\Delta_u$	0.1342	0.4135	0.4833	0.5063	R
$^4\Pi_g(1)$	0.3094	0.4850	0.5142	0.5205	R ?
$^4\Pi_g(2)$	0.1666	0.4393		0.5065	R
$^4\Pi_u(1)$	0.4414	0.5317	0.5312	0.5266	B
$^4\Pi_u(2)$	0.2985	0.4856		0.5124	R
$^4\Sigma_g^+$	0.5049	0.5743	0.5574	0.5402	B
$^4\Sigma_u^+$	0.1316	0.4126	0.4829	0.5062	R
$^4\Sigma_g^-(1)$	0.3799	0.5069	0.5202	0.5224	B ?
$^4\Sigma_g^-(2)$	0.1275			0.4946	R
$^4\Sigma_u^-(1)$	0.5789	0.5910	0.5613	0.5412	B
$^4\Sigma_u^-(2)$	0.2753	0.4656	0.4974	0.5037	R
$^2\Delta_g$	0.4375	0.5203	0.5171	0.5164	M
$^2\Delta_u$	0.5357	0.5666	0.5472	0.5331	B
$^2\Pi_g(1)$	0.6713	0.5937	0.5458	0.5284	B
$^2\Pi_g(2)$	0.2686	0.4706	0.5027		R
$^2\Pi_u(1)$	0.5604	0.5621	0.5359	0.5251	B
$^2\Pi_u(2)$	0.3484	0.4556	0.4945		R
$^2\Sigma_g^+(1)$	0.5042	0.5191	0.5166	0.5163	M
$^2\Sigma_g^+(2)$	0.4336	0.5034	0.4736	0.4595	B[O(^1D)]
$^2\Sigma_u^+$	0.5214	0.5628	0.5464	0.5329	B
$^2\Sigma_g^-(1)$	0.4885	0.5605	0.5469	0.5332	B
$^2\Sigma_g^-(2)$	0.3223		0.4996		R
$^2\Sigma_u^-(1)$	0.5111	0.5406	0.5247	0.5172	B
$^2\Sigma_u^-(2)$	0.2633		0.4998		R

[a] The designations B, R, M identify the state as bound, repulsive, or metastable with respect to the asymptote. The long-range character, i.e., beyond 6 a.u., of the energy curves is not considered in these designations.

TABLE VII. PNO-CI energy curves: GTF O$_2^-$.

	$-E = 149 +$ a.u.				
State	R 3.0	3.5	4.0	5.0	
$^4\Delta_g$	0.4754	0.5370	0.5468	0.5315	B
$^4\Delta_u$	0.0739	0.2895	0.3798	0.4489	R
$^4\Pi_g(1)$	0.2503	0.3846	0.4412	0.4764	R
$^4\Pi_g(2)$	0.1167	0.3282	0.4092	0.4630	R
$^4\Pi_u(1)$	0.3963	0.4754	0.4999	0.5043	R
$^4\Pi_u(2)$	0.2633	0.4202	0.4686	0.4911	R
$^4\Sigma_g^+$	0.4726	0.5353	0.5457	0.5311	B
$^4\Sigma_u^+$	0.0711	0.2878	0.3787	0.4485	R
$^4\Sigma_g^-(1)$	0.4432	0.5131	0.5289	0.5216	B
$^4\Sigma_g^-(2)$			0.3871	0.4470	R
$^4\Sigma_u^-(1)$	0.5515	0.5769	0.5685	0.5393	B
$^4\Sigma_u^-(2)$	0.2367	0.3822	0.4397	0.4738	R
$^2\Delta_g$	0.4006	0.4733	0.4910	0.4899	R
$^2\Delta_u$	0.5059	0.5415	0.5407	0.5218	B
$^2\Pi_g(1)$	0.6328	0.5883	0.5593	0.5188	B
$^2\Pi_g(2)$	0.2617	0.3878	0.4252	0.4443	R
$^2\Pi_u(1)$	0.5161	0.5265	0.5256	0.5078	B
$^2\Pi_u(2)$	0.3187	0.4065	0.4369	0.4531	R
$^2\Sigma_g^+(1)$	0.4662	0.4713	0.4893	0.4889	M
$^2\Sigma_g^+(2)$	0.3973	0.4665	0.4661	0.4494	B[O^1D]
$^2\Sigma_u^+$	0.4983	0.5419	0.5475	0.5349	B
$^2\Sigma_g^-(1)$	0.4544	0.5196	0.5321	0.5211	B
$^2\Sigma_g^-(2)$			0.4615	0.4819	R
$^2\Sigma_u^-(1)$	0.4727	0.5106	0.5096	0.5097	B
$^2\Sigma_u^-(2)$			0.4574	0.4778	R

Clearly the $^4\Delta_g$ and $^4\Sigma_g^+$ states, as an example, are bound. The prediction can hold only at distances very much greater than 6.0 a.u.

The CI description of these excited states and the significance of the states is best obtained by an analysis of the individual states; the states cannot be lumped together for such an analysis. Only a few states warrant such an analysis, and we have chosen the $X\,^2\Pi_g$, $^4\Sigma_u^-$, $^2\Pi_u$, $^2\Delta_u$, $^4\Delta_g$, $^2\Sigma_u^-$, and $^2\Sigma_g^+$ states.

$X\,^2\Pi_g$ State

Only three configurations are required to obtain formally correct dissociation of the $^2\Pi_g$ state.

However, the orbitals are not optimum for both neutral atom and ion, and the asymptotic energy that is approached is well above the HF energy[18] of the asymptote $O(^3P)+O^-(^2P)$. The asymptotic base configurations are the largest components of the wave function at $R = 6$ a.u., but the coefficient for the fourth configuration is already 0.14. Among the valence configurations the first four configurations are the most important over the range of distances studied.

The energy improvements obtained by adding the fourth configuration to the base configurations is 0.0031, 0.0133, 0.0368, and 0.04518 a.u. for 6, 5, 4, and 3 a.u., respectively, in the MC-SCF results. The configurations's increasing importance reflects the uncoupling of the atomic electrons on the neutral atom or the increasing importance of atom configurations coupled ^1D. The configurations that asymptotically describe the $^2\Pi_g(2)$ state that correlated with the $O^-(^2P)+O(^3P)$ asymptote, do not mix significantly at any distance with the base for $^2\Pi_g(1)$ or with the fourth configuration. There is no valence mixing which will lead to an attractive excited state of $^2\Pi_g$ symmetry.

The PNO-GTF results yield results that are similar but energetically inferior to the MC-SCF-STF values as expected. The relative weights of the configurations are quite comparable as can be seen by comparison from the coefficients for the important four configurations at 5.0 and 3.0, respectively. The values for the MC-SCF calculation for $R = 5.0$ and 3.0, respectively, are 0.826, -0.394, 0.302, and 0.239 and 0.954, -0.172, 0.054, and 0.233, while for the PNO calculation they are 0.837, -0.390, 0.282, and 0.247 and 0.900, -0.275, 0.143, and 0.295. The differences cannot be easily analyzed and since the MC-SCF results are generally superior, they will be discussed alone.

$^4\Sigma_u^-$ *States*

As in the case of the ground state the configurations for the two $^4\Sigma_u^-$ states at 6 a.u. are already significantly perturbed from the base configuration coefficients. This observation is in accord with the lack of correlation of the calculated energies of all the negative-ion states with the predictions of long-range perturbation theory. For all the excited states the calculations reported here represent the intermediate and equilibrium range of distances. The coefficients of the base configurations are recognizable at 6.0 a.u., but there are always substantial differences from the asymptotic values.

The minimum for this state is in the neighborhood of 3.5 a.u., but even at 3.0 a.u. the coefficients of the three valence configurations are 0.939, 0.187, and -0.303. The excited states of O_2^- are stable at large internuclear separation and, primarily due to the necessity of a MC description required for formally correct dissociation, the states themselves must be described by a number of configurations. The results for the $^4\Sigma_u^-$ state are true for all the negative-ion states that require a MC description asymptotically.

The configurations required in addition to the first dominant HF configurations have increased $3\sigma_u$ occupancy for configuration 2 and increased $1\pi_g$ occupancy for configuration 3. Since the antibonding characteristics of these orbitals are reduced with increasing atomic separation, their importance at these distances should occasion no surprise. Even more significantly the occupancy of the $3\sigma_u$ orbital is now slightly greater than one which helps to keep the orbital from getting diffuse. Even at 3 a.u. the $3\sigma_u$ orbital shows little tendency toward diffuseness; at these distances it can be described in united atom terms as a promoted $4f\sigma$ or $4p\sigma$ but still compressed within the HF molecular size and acting as a correlation orbital. Since the neutral $^3\Sigma_g^-$ HF configuration of O_2 is not lower in energy than this state for the same basis set, it is not possible to have a solution for which HF configuration has a coefficient of 1.0 and the $3\sigma_u$ molecular orbital is determined to be a constant. Therefore, the MC-SCF results at the distances considered do not have tendencies toward such an autodetached solution since the coefficients for functions with the smallest exponents do not dominate the $3\sigma_u$ orbital. At shorter internuclear separation the HF function will increasingly dominate, and the inclusion of diffuse trial functions will lead to a neutral molecule and a constant $3\sigma_u$. Autodetachment would lead to an enhancement of excited vibrational energy levels of the ground state at the energy of the resonance as recently proposed by Hasted[19] and observed by Trajmar *et al.*[20]

$^2\Pi_u$ *State*

The $^2\Pi_u$ excited state has the same correlation behavior as the $X\,^2\Pi_g$ state. The relative bonding behavior of the HF configuration 1 essentially determines the excitation energy of the $^2\Pi_u$ relative to $X\,^2\Pi_g$. Since the HF configuration is relatively higher in energy the singlet-coupled split-shell excitation determined by configuration 4 is relatively more important for the $^2\Pi_u(1)$ state than for $X\,^2\Pi_g$. In fact all the valence-correlating configurations have larger coefficients for $^2\Pi_u(1)$ as compared with $X\,^2\Pi_g$.

The equilibrium internuclear separation for the $^2\Pi_u$ state is between 3 and 3.5 a.u., where the HF configuration has a coefficient greater than 0.9. Relative to the neutral HF ground state $X\,^3\Sigma_g^-$ the HF configuration for $^2\Pi_u(1)$ is obtained by excitation of $1\pi_u^4 1\pi_g^2 \rightarrow 1\pi_u^3 1\pi_g^3$ with subsequent attachment to the $1\pi_g$ orbital of the excited configuration. Since the attached electron has significant bonding properties, this valence-type Feshbach negative-ion resonance state does not have an energy curve similar to its parent, as is the case of Rydberg attachment states.[21] At internuclear separations greater than 3 a.u. the stability of the valence-type Feshbach state is in part due to the large affinity of the oxygen atom. This state is weakly bound and its asymptote is well below the respective neutral asymptote. The excitation energy between the equilibrium positions of the $X\,^2\Pi_g$ state, defined by a linear combination of valence states and a similarly described $^2\Pi_u(1)$ state, is about 3.8 eV. This would be in reasonable agreement with the short-wavelength limit of the single progression observed by Rolfe[3(a)] at about 3.65 eV. Extrapolation of the $^2\Pi_u(1)$ energy curve to shorter distances shows that this state, the $^2\Sigma_g^+$ state, and the $^4\Sigma_u^-(1)$ state are the only ones for which the left-hand lines intersect the Franck–Condon region of the $v=0$ vibration of the neutral ground state. Electron attachment with dissociation has been assigned to a $^2\Pi_u$ state from the observed angular distribution of the fragments[4]; the energy curve for this state is at the required energy, as has been long anticipated.[5,6] As Hasted[19] has noted, decay from this resonance state can also yield excitation of a vibrationally excited $^3\Sigma_g^-$ state and the electronically excited $^1\Delta_g$ and $^1\Sigma_g^+$ states.

The $X\,^2\Pi_g$ to $X\,^2\Pi_u$ transition of O_2^- may also be related to the transition near 2000 Å observed in HO_2.[22] The geometry of the ground state of HO_2 is found[23] to be consistent with interpreting the electronic structure as $H^+O_2^-$. Since the $^2\Pi_u$ state dissociates to $O^- + O$ it is a strong presumption that the analogous transition in HO_2 yields OH and O products.

$^2\Delta_u$, $^2\Sigma_u^-$, $^2\Sigma_u^+$ *States*

There are two obvious groups of relatively low-lying excited states to be considered in addition to the $^4\Sigma_u^-$ and $^2\Pi_u$. The first set arises from different couplings of the molecular orbitals occupied identically to the HF configuration of the $^4\Sigma_u^-$. This would include $^2\Delta_u$, $^2\Sigma_u^-$, and $^2\Sigma_u^+$ states. The second set corresponds to attachment of an electron to the $3\sigma_u$ orbital subsequent to excitation of the $1\pi_u$ electron to the $1\pi_g$ orbital. Out of this set we will consider the $^4\Sigma_g^+$, $^2\Delta_g$, $^2\Sigma_g^-$, and $^2\Sigma_g^+$ states below.

The $^2\Delta_u$, $^2\Sigma_u^-$, and $^2\Sigma_u^+$ states have equilibrium internuclear separations between 3.5 and 4.0 a.u. All states show strong mixing between the HF configuration and the configuration with $\Pi_u^2\Pi_g^4$ occupancy. It is this mixing which determines that the state is below the $^2\Sigma_u^-$ state and almost as low in energy as the $^2\Delta_u$ state. There is also appreciable mixing in all three states of the $3\sigma_g 1\pi^3(^1\pi)1\pi_g^3$ configuration as well as considerable persistence of the asymptotic configurations into relatively short distances.

$^4\Sigma_g^+$, $^2\Delta_g$, $^4\Sigma_g^-$, $^2\Sigma_g^+$ *States*

The $^4\Sigma_g^+$ state is determined by only one configuration as are the $^4\Delta$ states for which the spin and angular momentum are maximum. Such states are very useful to generate bases for input to the MC-SCF as long as the physical interaction does not distort these systems too much relative to the other states. At large distances there is little difference in orbitals which simply reconstruct distorted atoms; for these ions the $^4\Delta_g$ is bound and again the orbitals are useful representatives of the bound valence states.

The $^4\Sigma_g^+$ and $^4\Delta_u$ differ only in a small-exchange integral and the energy curves are essentially congruent. These quartet states have the second and third largest T_e values but both are rising rapidly as the R_e of the neutral state is approached.

The dominant HF configurations of the $^2\Delta_g$ state are the third and fourth in Table IV, since the $3\sigma_u$ orbital is very antibonding. This is true for the $^2\Sigma_g^-$ state as well. Again no sc dominates at $R=4.0$ a.u. At shorter distances these states are very high in energy relative to the dissociative asymptote and will not play any role in the absorption or associative dissociation processes of interest.

The $^2\Sigma_g^+$ states are also relatively high in energy, which shows the importance of a CI description. As noted earlier the third $^2\Sigma_g^+$ configuration is apparently one of the low-lying excited states in the HF approximation. However, that configuration turns out to be the dominant one for the *second* root of the secular equation at internuclear separations greater than 4 a.u.; this state correlates with $O^-(^2P)+O(^1D)$. However, at 3.0 a.u. the levels have switched and the adiabatic energy curve is distorted in this region. The $^2\Sigma_g^+(1)$ curve is trending toward lower energies at distances shorter than 3 a.u. From Fig. 2 the $^2\Sigma_g^+(1)$ energy curve would extrapolate to the third highest excited state after the $^4\Sigma_u^-$ and $^2\Pi_u$ states. Dissociation from this state would require, however, a curve crossing and the state should not be important in excitation processes.

IV. CONCLUSION

Configuration-interaction calculations that provide for formally correct dissociation have revealed a number of bound states of O_2^-. All of the excited states are found to have equilibrium internuclear separations at least 1 a.u. larger than the ground state. This results necessarily from the antibonding excited valence molecular orbitals required to construct the negative-ion configurations. Nonetheless, in addition to the $X\,^2\Pi_g$ ground state, there are two states that probably play a role in low-energy (ca. 4–5 eV) resonance attachment to the ground state. They are the $^4\Sigma_u^-$ and $^2\Pi_u$ states which can be characterized, respectively, as shape and valence Feshbach resonances. Since the valence excited orbitals are quite antibonding, the $^2\Pi_u$ resonance-state energy curve is not similar to any of the energy curves of the parent molecular-orbital configuration $1\pi_u^3 1\pi_g^3$. We would certainly expect analogous molecular ion states for other diatomic molecules both homonuclear and heteronuclear including molecules such as N_2[24] and CO, even though these molecules do not have bound negative-ion states with respect to the neutral ground state.

The calculation of these excited ion states can be done relatively simply with valence configurations mixed in the MC-SCF method. As noted earlier, correlation effects should become more important at shorter internuclear separations. But the ion-multipole, multipole-multipole, exchange coupling, and charge-transfer effects are already included at the OVC level and these effects dominate the intermediate range where these states are bound.

---

*Supported in part by NASA.

†Supported in part under the auspices of the U. S. Atomic Energy Commission.

[1] R. J. Celotta, R. A. Bennett, and J. L. Hall, in *Proceedings of the Seventh International Conference on Physics of Electronic and Atomic Collisions* (North-Holland, Amsterdam, 1971), p. 179; R. J. Celotta, R. A. Bennett, J. L. Hall, M. W. Siegel, and J. Levine, Phys. Rev. A 6, 631 (1972).

[2] W. T. Zemke, G. Das, and A. C. Wahl, Chem. Phys. Letters 14, 310 (1972).

[3] (a) J. Rolfe, J. Chem. Phys. 40, 1664 (1964); (b) W. Holzer, W. F. Murphy, H. J. Bernstein, and J. Rolfe, J. Mol. Spectry. 26, 543 (1968).

[4] R. J. Van Brunt and L. J. Kieffer, Phys. Rev. A 2, 1899 (1970).

[5] T. F. O'Malley and H. S. Taylor, Phys. Rev. 176, 207 (1968).

[6] (a) H. S. W. Massey, *Negative Ions* (Cambridge U. P., Cambridge, England, 1950); (b) R. S. Mulliken, Phys. Rev. 115, 1225 (1959).

[7] (a) M. Krauss, A. C. Wahl, and W. Zemke, in *Proceedings of the Seventh International Conference on Physics of Electronic and Atomic Collisions* (North-Holland, Amsterdam, 1971), p. 1168; (b) H. H. Michels and F. E. Harris, *ibid.*, p. 1170.

[8] A. C. Wahl and G. Das, Advan. Quantum Chem. 5, 261 (1970).

[9] C. Edmiston and M. Krauss, J. Chem. Phys. 45, 1833 (1966).

[10] C. C. J. Roothaan, Rev. Mod. Phys. 32, 179 (1960).

[11] H. S. Taylor and F. E. Harris, J. Chem. Phys. 39, 1012 (1963).

[12] (a) J. N. Bardsley, F. Mandl, and A. R. Wood, Chem. Phys. Letters 1, 359 (1967); (b) M. Krauss and F. H. Mies, Phys. Rev. A 1, 1592 (1970).

[13] The STF calculation used BISON, "a Fortran computer system" by A. C. Wahl, P. J. Bertoncini, K. Kaiser, and R. H. Land [ANL Report No. ANL-7271, 1968 (unpublished)]; and Intern. J. Quantum Chem. 35, 499 (1970)].

[14] The GTF calculation used IBMOL: Version 2, E. Clementi and A. Veillard, IBM Research Lab. Report (1966). IBMOL/2 was modified at the National Bureau of Standards for the present open-shell problem. IBMOL description is given by E. Clementi and D. R. Davis [J. Comp. Phys. 2, 223 (1967)].

[15] T. L. Gilbert and P. S. Bagus's (unpublished) atom bases which are partially tabulated in Ref. 13.

[16] S. Huzinaga, J. Chem. Phys. 42, 1293 (1965).

[17] W. J. Stevens and F. B. Billingsley, II (private communication).

[18] E. Clementi and A. D. McLean, Phys. Rev. 133, A419 (1964).

[19] I. W. Larkin and J. B. Hasted, J. Phys. B 5, 95 (1972).

[20] S. Trajmar, D. C. Cartwright, and W. Williams, Phys. Rev. A 4, 1482 (1971).

[21] A. W. Weiss and M. Krauss, J. Chem. Phys. 52, 4363 (1970).

[22] (a) G. Czapski and L. M. Dorfman, J. Phys. Chem. 68, 1169 (1964); (b) S. Gordon, E. J. Hart, and J. K. Thomas, J. Phys. Chem. 68, 1262 (1964); (c) G. Czapski and B. Halpeim, Israel J. Chem. 5, 185 (1967); (d) J. Rabani and S. V. Nielsen, J. Phys. Chem. 73, 3736 (1969); (e) C. J. Hochanadel, J. A. Ghormley, and P. J. Ogren, J. Chem. Phys. 56, 4426 (1972).

[23] (a) M. E. Jacox and D. E. Milligan, J. Mol. Spectry. (unpublished); (b) the radical HNO was also calculated to be essentially H^+NO^- by M. Krauss [J. Res. Natl. Bur. Std. (U.S.) 73A, 191 (1969)].

[24] Band *a* in the electron transmission spectra of N_2 reported by L. Sanche and G. J. Schulz [Phys. Rev. A 6, 69 (1971)] probably results from attachment to a parent molecular-orbital configuration, $1\pi_u^3\, 1\pi_g$, as postulated by Sanche and Schulz.